



**Shiraz University
Faculty of Science**

Ph.D. Dissertation in Optics and Lasers

**THE EFFECTS OF THERMALLY INDUCED HEAT
ON SPECIAL TYPES OF LASER BEAMS**

**By
MOJTABA SERVATKHAH**

**Supervised by
Dr. HAMID NADGARAN**

December 2011

In The Name

of

God

The

Merciful

The

Compassionate

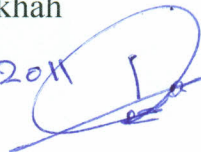
IN THE NAME OF GOD

DECLARATION LETTER

I, **Mojtaba Servatkah**, a Physics student majored in Optics and Lasers from the Faculty of Physics declare that this thesis is the result of my research and I have written the exact reference and full indication whenever I used other's sources. I also, declare the research and the topic of my thesis are not reduplication and guaranty that I will not disseminate its accomplishments and not make them accessible to others without the permission of the university according to the regulations of the mental and spiritual ownership. All rights of this thesis belong to Shiraz University.

Mojtaba Servatkah

Date: 21, 12, 2011



IN THE NAME OF GOD

THE EFFECTS OF THERMALLY INDUCED HEAT ON
SPECIAL TYPES OF LASER BEAMS

BY

MOJTABA SERVATKHAH

THESIS

SUBMITTED TO THE SCHOOL OF GRADUATE STUDIES IN PARTIAL
FULFILLMENT OF THE REQUIREMENTS FOR THE DEGREE OF DOCTOR
OF PHYLOSOPHY (Ph.D.)

IN

PHYSICS

SHIRAZ UNIVERSITY

SHIRAZ

ISLAMIC REPUBLIC OF IRAN

EVALUATED AND APPROVED BY THE THESIS COMMITTEE AS: EXCELLENT

H. Nadgar H. NADGARAN, Ph.D., ASSOC. PROF. OF PHYSICS
(CHAIRMAN)
M. M. Golshan M. M. GOLSHAN, Ph.D., ASSOC. PROF. OF PHYSICS
A. Zakeri A. ZAKERI, Ph.D., PROF. OF PHYSICS
M. Hosesini Farzad M. HOSESINI FARZAD, Ph.D., ASSIS. PROF OF
PHYSICS
~~*H. R. Fallah* H. R. FALLAH, Ph.D., ASSOC. PROF. OF PHYSICS
(EXTERNAL EXAMINER)~~

DECEMBER 2011

To

My Parents, My Sister

&

Specially My Wife

Acknowledgements

This thesis would not have been possible without the guidance and the help of several individuals who contributed and extended their valuable assistance in the preparation and completion of this study.

First and foremost, my utmost gratitude goes to Dr. H. Nadgaran, whose encouragement, supervision and support, from the preliminary to the concluding levels, enabled me to develop an understanding of the subject.

The members of my thesis committee, Dr. A. Zakeri, Dr. M. Hosseinifarzad Dr. A. Pustfrush and the external examiner, Dr. H. R. Fallah (Physics Department, Isfahan University, Isfahan, Iran) for their fruitful suggestions, specially Dr. M. M. Golshan for all his advice, encouragement and valuable suggestions. I am also greatly indebted to all my professors in Physics Department of Shiraz University.

I gratefully acknowledge Dr. M. Sabaeian for his advice and constructive comments on the subject of this thesis.

Most of all I am indebted and thankful to my parents and my wife for their abundant support. Their encouragement and advice will always be remembered.

ABSTRACT

The Effects of Thermally Induced Heat on Special Types of Laser Beams

BY:

Mojtaba Servatkah

Thermal effects play an important and crucial role in laser's beam quality and beam profile alteration. Since recognition and discrimination of thermally affected laser beams from their pure, and standard non-thermal counterparts is very important in practice, it is necessary to discuss the propagation of various special form of laser beams in inhomogeneous thermal lens media.

The main aim of this work is to present a thermal model addressing thermally-affected Mathieu-Gauss (MG) and Ince-Gauss (IG) beams.

In doing so, we use a thermal model to simulate the beam profile of zero-order MG beams and compare it with the non-thermal beam profile. The results not only support the justification of the thermal effects importance, but also demonstrate that these effects are so pronounced, that MG beam identification at some high pump powers is indeed difficult.

In Ince-Gaussian case, the results show considerable beam spot size variations for near fields under various induced heat loads. As Ince-Gaussian beams are directly related to cavity symmetry breaking, the results can greatly help system designers for circumventing these types of symmetry breaks usually encountered in high power lasers.

To model the induced heat loads, we consider two types of power input, namely, Gaussian and super-Gaussian profiles. As for the out-put laser

beam, MG and IG beams with different modes, are considered and their respective intensity profiles are plotted. We show that:

Near field profiles, for both the MG and IG beams, remain intact with small (large) contractions for small (large) power inputs. The far field profiles, on the other hand suffer drastic changes: The side lobes disappear giving rise to central ones.

Table of Contents

Chapter 1 Introduction

Motivation.....	2
-----------------	---

Chapter 2 Literature Survey

2.1 A Historical Review of Thermo Optic Effects in Diode-Pumped Solid State Lasers.....	7
2.2 A Historical Review of Special Types of Laser Beams	11

Chapter 3 Thermo-Optic effects in Diode-Pumped Solid State Lasers

3.1 Introduction.....	17
3.2 Heat Equation, Initial and Boundary Conditions	18
3.2.1 General Heat Equation	18
3.2.2 Boundary Conditions	21
3.3 Thermal lens effects.....	22
3.3.1 Introduction.....	22
3.3.2 dn/dT Effect.....	22
3.3.3 End Effect	23
3.3.4 Depolarization Loss	23
3.4 Thermal Model.....	24
3.4.1 ABCD Transfer Matrix of a Thermally-Induced Lens-Like Medium	27
3.4.2 Nd:YAG Crystal	29

Chapter 4 Special Types of Laser Beams

4.1 Introduction.....	32
-----------------------	----

4.2 Helmholtz-Gauss Beams	33
4.2.1 Cosine-Gauss Beams.....	36
4.2.2 Bessel-Gauss Beams	37
4.2.3 Parabolic-Gauss Beams.....	39
4.2.4 Mathieu-Gauss Beams	40
4.2.5 MG Beams Propagating Through an ABCD Optical System.....	47
4.3 Paraxial Beams.....	49
4.3.1 Hermite-Gaussian Beams.....	50
4.3.2 Laguerre-Gaussian Beams	52
4.3.3 Ince-Gaussian Beams	53
4.3.4 IG Beams Propagating Through an ABCD Optical System.....	56

Chapter 5

Effects of Induced Heat Loads on Special Types of Laser beams

5.1 Introduction.....	59
5.2 Thermally Affected Mathieu-Gauss Beams	60
5.3.1 Results and Discussions.....	63
5.4 Thermally Affected Ince-Gaussian Beams	81
5.5.1 Results and Discussion	81

Chapter 6

Conclusion

6.1 Mathieu-Gauss Beams	99
6.2 Ince-Gaussian Beams	100

References	102
-------------------------	-----

List of Figures

Figure 1-1	Schematic illustration of an end pumped Nd:YAG laser	4
Figure 3-1	Three-dimensional heat conduction through a rectangular volume element (left), and three-dimensional volume element in cylindrical coordinates (right).....	18
Figure 3-2	Combination of conduction, convection and radiation heat transfer.....	21
Figure 3-3	Absorption coefficient of Nd:YAG crystal versus wavelength	29
Figure 4-1	Transverse intensity pattern of Cosine-Gauss beams.....	37
Figure 4-2	Transverse intensity pattern of Bessel-Gauss beam	38
Figure 4-3	Transverse intensity pattern of Parabolic-Gauss beam	40
Figure 4-4	Elliptical-cylindrical coordinate	41
Figure 4-5	Transverse intensity pattern of Mathieu-Gauss beam	47
Figure 4-6	Transverse intensity distribution pattern of Gaussian beam.....	50
Figure 4-7	Transverse intensity distribution of different modes of Hermite-Gauss beam.....	51
Figure 4-8	Transverse intensity distribution of different modes of Laguerre-Gaussian beam.....	53
Figure 4-9	Transverse field distributions of several low-order IG beams a) even, b) odd for $\epsilon=2$	56
Figure 5-1	a) Crystal temperature distribution versus r and b) versus z for 1W, 2W, 3W, 4W and 5W pump power from bottom to top.	61
Figure 5-2	a) Crystal Refractive index versus r and b) versus z for 1W, 2W, 3W, 4W and 5W pump power from bottom to top.....	62
Figure 5-3	Non-thermal and thermally-affected MG beam intensity profile at $z_2=2\text{cm}$. a) Under pump power of 1W. b-e) Under pump powers of 2W, 3W, 4W, and 5W, respectively. Solid plots represent the non-thermal beam, dotted plots show the MG beam under super-Gaussian pump, and dashed plots depict the MG beam under Gaussain pump. Dark pictures is the transverse pattern on XY plane together with their 3D plots.	68

Figure 5-4 The same as Fig. 5-3, but at $z_2=5\text{cm}$	74
Figure 5-5 The same as Fig. 5-3, but at $z_2=40\text{cm}$ (far field).....	80
Figure 5-6 Two different ABCD output of IG beams under various induced heat loads (columns from left: Nonthermal, 1W, 3W and 5W induced heats) and various distances from the laser aperture (rows: at 2cm, 5cm and 40cm).	83
Figure 5-7 Two more different ABCD output of IG beams under different induced heat loads and various distances from the laser aperture (rows: at 2cm, 5cm and 40cm).	84
Figure 5-8 ABCD output of odd IG beams Rows and columns are the same as in Fig. (5) and in Fig. (6).....	85
Figure 5-9 ABCD output of MG beams under different induced heat loads (columns from left: Nonthermal, 1W, 3W and 5W induced heats) and various distances from the laser aperture (rows: at 2cm, 5cm and 40cm)	86
Figure 5-10 Two dimensional beam profile for $IG_{2,0}^e$ a) $z_2=5$ cm and b) $z_2=40$ cm. The profiles are shown by different colors and different induced heat powers at $\theta = 90^\circ$ (on the y axis).	88
Figure 5-11 Two dimensional beam profile for $IG_{1,1}^e$ a) $z_2=5$ cm and b) $z_2=40$ cm at $\theta = 0^\circ$ (on the x axis).....	89
Figure 5-12 Two dimensional beam profile for $IG_{2,2}^e$ a) $z_2=5$ cm and b) $z_2=40$ cm at $\theta = 0^\circ$ (on the x axis).....	91
Figure 5-13 Two dimensional beam profile for $IG_{4,2}^e$ a) $z_2=5$ cm and b) $z_2=40$ cm at $\theta = 0^\circ$ (on the x axis).....	92
Figure 5-14 Two dimensional beam profile for $IG_{4,4}^o$ a) $z_2=5$ cm and b) $z_2=40$ cm at $\theta = 30^\circ$ (with respect to x axis).....	93
Figure 5-15 Two dimensional beam profile for $IG_{1,1}^o$ a) $z_2=5$ cm and b) $z_2=40$ cm $\theta = 90^\circ$ (on the y axis).....	94
Figure 5-16 $z_2=2$ cm Two dimensional beam profiles for a) $IG_{2,0}^e$ at $\theta = 90^\circ$ b) $IG_{1,1}^e$ at $\theta = 0^\circ$ c) $IG_{2,2}^e$ at $\theta = 0^\circ$ d) $IG_{4,2}^e$ at $\theta = 0^\circ$ e) $IG_{4,4}^o$ at $\theta = 30^\circ$ f) $IG_{1,1}^o$ at $\theta = 90^\circ$ (θ is the angle with respect to x axis).....	97

Chapter 1

Introduction

Motivation

Any change in the refractive index of a laser active medium can lead to serious degradation of beam quality, laser beam modes, laser performance and variation in the intensity distribution. Alteration in the refractive index of laser active medium is especially notable in high power lasers. It is clear that in the laser beam production, the pumping agent induces a great amount of heat which is loaded on the laser active medium. This induced heat load, subsequently the induced change of refractive index, is enormous. Heat load in laser active medium can, at least in certain circumstances, switch the stable laser resonator to an unstable one. Besides, highly heated crystals (laser active media) pose serious technical and maintenance problems. Another effect of induced heat load on laser crystals is the induced stress within the crystal. Stress can deform the crystal so that another considerable change of refractive index is faced by the crystal. The non-uniform heating of laser active medium leads to non-uniform index of refractive index. Such medium is named graded index (GRIN) medium. Therefore, these inductions must well be taken into account when one is dealing with design and construction of high power lasers.

Special types of laser beams are very much attractive in various scientific and industrial applications. This thesis is devoted to an investigation on the generation and propagation of these special types of laser beams, namely Helmholtz-Gauss and Paraxial beams in a GRIN medium that appears as a result of a highly suffered medium from induced heat load. The procedure with which this goal is achieved will be given shortly. The more important results of our investigation, however, are briefly discussed presently.

1. The induced heat load causes the change in the refractive index of laser active medium. This change in turn induces a thermal lens in the medium.
2. The focal length of thermally induced lens decreases with increasing the power of pumping agent.
3. The change in MG output profile is almost independent of the two types of input power distributions used in this work (Gaussian and super Gaussian).
4. Increasing the power of pumping agent causes contraction of the near field MG beam intensity profile without changing its shape.
5. At $z=5$ cm which is chosen as a measure of middle field, by increasing the power of input power, the intensity profile contract and the central lobe disappears giving rise to the side lobes.
6. The far field profiles show the appearing of the central lobe along with disappearing of the side ones due to increasing of the pump power.
7. In case IG beams the effect of increasing the pump power is the contraction of the near field intensity profiles without changing their shape for different modes of these beams.
8. The middle field intensity profiles of the modes with central lobe suffer two types of change: contraction of the profile and disappearing of the central lobe giving rise to the side ones.
9. The middle field intensity profiles of the modes without central lobe just contract with increasing the pump power.
10. Increasing of the pump power cause the disappearing of the side lobes and appearing of the central ones in the case of the far field intensity profiles of IG beams with central lobe.
11. The effect of increasing the pump power on the far field profile of IG beams without central lobe is just the contraction or expansion of the profile.

The aforementioned procedure now follows.

In chapter 2 a detailed review of the literature including a historical outline of thermo-optical effects in diode-pumped solid state lasers and a historical view of special types of laser beams will be presented. In particular, a thorough review of The history of the development of the MG and IG beams are also presented in this chapter.

In order to model the effects of induced heat load on the propagation of special types of laser beams we consider a laser system which produces Mathieu-Gauss or Ince-Gaussian beams. A schematic illustration of the laser system is shown below:

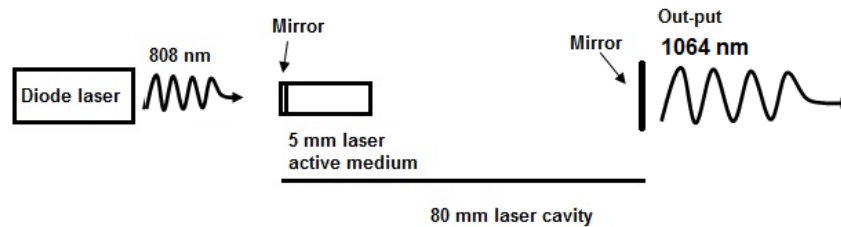


Figure 1-1 Schematic illustration of an end pumped Nd:YAG laser

As shown in the illustration, a diode laser with central wavelength of 808 nm is used as the pumping agent. A 5 mm long, Nd:YAG crystal with 1.5 mm radius is used as the laser active medium. Maximum absorption of the crystal is at about 808 nm, the central wavelength of the pumping agent.

One end of the laser crystal is coated so as to act as one mirror of the laser cavity. Another mirror is placed 80 mm in front of the first one. So the laser free length is 75 mm. The out-put laser beam is a Mathieu-Gauss or Ince-Gaussian beam with central wavelength of 1064 nm. At this wavelength the laser active medium is transparent, so the only source of generating heat in the laser crystal is the induced heat of the pumping agent.

Taking the above considerations into account, chapter 3 presents a detailed study of heat equation. Taking the induced heat loads as sources we solve the heat equation, giving the temperature as a function of position. A discussion of the effects of temperature (as a function of position) on the refractive index is also presented in this chapter. A thermal model for lensing effects, along with the corresponding ABCD transfer matrix, for an Nd:YAG laser, are also presented in this chapter.

Since the central part of this research is comprised of Mathieu-Gauss and Ince-Gaussian beams, as the outputs of a solid state laser, suffered from the induced heat loads, chapter 4 is devoted to a discussion of such laser beams. The

properties of their generation and propagation through an ABCD optical systems, is also reviewed in this chapter.

In chapter 5, use is made of the temperature distributions, as calculated in the third chapter, to investigate the effects of input power. Since the shape of the output beams is of considerable interest, we further investigate these profiles of different locations on the cavity axis, with due attention to the input power. The procedure and the results are also given in this chapter.

This thesis is concluded in chapter 6 with an outline of the results, some further remarks and some proposals for future works.

Chapter 2

Literature Survey

2.1 A Historical Review of Thermo Optic Effects in Diode-Pumped Solid State Lasers

Increasing demands for high power lasers for everyday use in different aspects of human life including industries, medical, communications and so on, have made the study of thermally induced effects on the output of these lasers inevitable.

The first experimental record of thermal lensing effect goes back to Gordon *et al.* (1965) [1]. They observed build-up and decay of thermal lensing when polar or nonpolar liquid cells were placed within the resonator of a helium-neon laser operating at 6328 Å. They believed that the effects were caused by absorption of the red light in the material, producing a local heating at the vicinity of the beam and a lens effect arising from the transverse gradient of refractive index.

In 1966 Quelle [2] investigated thermal effects and the relative sensitivity of a variety of materials to nonuniform energy depositions. Osterink *et al.* [3] increased the volume of fundamental transverse mode of a CW power laser by compensating the thermal lens effect of its Nd:YAG rod. They obtained over 1.4 W in the TEM₀₀ mode, compared to about 200–300 mW without compensation. Koechner [4] used the theory of interaction of a linearly polarized wave with a continuously pumped Nd:YAG crystal to illustrate the angular independency of birefringence, though the radial dependence, and explained the laser power losses involved.

Experimental studies on the mechanisms that cause amplitude modulation in CW-pumped YAG lasers were also performed by Koechner in 1970 [5]. In that work the amplitude of modulation and frequency spectrum of the laser output fluctuations of a commercially available Nd:YAG laser were measured. It was found that by performing several modifications on the laser system, the output fluctuations were reduced by two orders of magnitude. In 1973 [6], he derived

expressions for the transient temperature distribution in optically pumped cylindrical laser rods for single-shot and repetitively pulsed operations and for both solid and hollow cylindrical laser rods. Hu *et al.* [7] suggested a simple and sensitive method of measuring the thermally induced index changes arising from absorption of a laser beam by a low-loss material. In their method, the sample was placed outside the laser cavity at the position of minimum radius of curvature of the wavefront that is at focal distance behind the beam waist. The method was sensitive enough to measure absorption coefficients of the order of $5 \times 10^{-6} \text{ cm}^{-1}$. Although the method was illustrated for the realization of thermal effects, it was applicable to other nonlinear index changes induced by laser beams. In 1983 Sheldon *et al.* [8] derived a theoretical model for the laser-induced thermal lens effect in weakly absorbing media. The model predicted the intensity variation of the laser beam in the presence of the lensing medium at far field, taking into account the aberrant nature of the thermal lens. In 1985, Greninger *et al.* [9] presented a general optical model which could predict optical wave front distortions and birefringence due to stress and temperature variations in laser heated and pressure loaded windows for cubic lattice materials. They also presented a computer code that integrated stress and thermal computations with an optical model to predict the wave front distortions. Power (1990) [10] proposed a model using Fresnel diffraction for dual beam pulsed laser thermal lens effect detection. The model accommodated the effects of aberrations in the lens element introduced by departures of the sample's thermally induced refractive index profile from the ideal parabolic approximation. It also used probe and irradiation beams of arbitrary complex radius at the sample position, and permits the computation of probe beam intensity profiles observed at arbitrary cell-detector distances. Shen *et al.* [11] presented a theoretical model for a CW laser induced thermal lens spectrometry taking the aberrant nature of thermal lens into account in 1992. Their model is suitable for mode-mismatched, mode-matched dual-beam and single-beam methods. Farrukh *et al.* (1998) [12] [13] derived an expression for the time-dependent temperature distribution in a finite solid-state laser rod, for an arbitrary distribution of pump energy. They used this formulation to predict the time evolution of temperature in Ti:Sapphire laser rods and in Nd:YAG ones.